

6-1-2008

# Lithography on GaP(100) surfaces

Rosangelly Flores-Perez

*Purdue University - Main Campus, rflores@purdue.edu*

Dmitry Zemlyanov

*Birck Nanotechnology Center, Purdue University, dimazemlyanov@purdue.edu*

Albena Ivanisevic

*Birck Nanotechnology Center, Purdue University, albena@purdue.edu*

Follow this and additional works at: <http://docs.lib.purdue.edu/nanopub>



Part of the [Nanoscience and Nanotechnology Commons](#)

---

Flores-Perez, Rosangelly; Zemlyanov, Dmitry; and Ivanisevic, Albena, "Lithography on GaP(100) surfaces" (2008). *Birck and NCN Publications*. Paper 332.

<http://docs.lib.purdue.edu/nanopub/332>

This document has been made available through Purdue e-Pubs, a service of the Purdue University Libraries. Please contact [epubs@purdue.edu](mailto:epubs@purdue.edu) for additional information.



## Lithography on GaP(100) surfaces

Rosangelly Flores-Perez<sup>a</sup>, Dmitry Y. Zemlyanov<sup>b</sup>, Albena Ivanisevic<sup>a,c,\*</sup>

<sup>a</sup> Department of Chemistry, Purdue University, West Lafayette, IN 47907, United States

<sup>b</sup> Birck Nanotechnology Center, Purdue University, West Lafayette, IN 47907, United States

<sup>c</sup> Weldon School of Biomedical Engineering, Purdue University, West Lafayette, IN 47907, United States

### ARTICLE INFO

#### Article history:

Received 7 February 2008

Accepted for publication 2 April 2008

Available online 8 April 2008

#### Keywords:

Gallium phosphide

Atomic force microscopy

X-ray photoelectron spectroscopy

Infrared spectroscopy

Microcontact printing ( $\mu$ CP)

dip-pen Nanolithography (DPN)

### ABSTRACT

Two types of lithographic methods were used to modify GaP(100) surfaces with commercially available alkanethiol molecules: microcontact printing ( $\mu$ CP) and “dip-pen” nanolithography (DPN). The patterned surfaces were characterized by atomic force microscopy (AFM), X-ray photoelectron spectroscopy (XPS) and Fourier transform infrared reflection absorption spectroscopy (FT-IRRAS). The characterization was done in order to understand the quality of each type of pattern, its chemical composition, and the organization of the molecules on the surface. Differences between the two lithographic methods used to do lithography on the GaP(100) in this study were dependent on the chosen molecular “ink”.

© 2008 Elsevier B.V. All rights reserved.

### 1. Introduction

Numerous researchers have utilized lithographic approaches in order to address problems with variable complexity [1,2]. In recent decades, patterning techniques such as microcontact printing ( $\mu$ CP) and “dip-pen” nanolithography (DPN) have been used on various materials and have utilized a number of molecular “inks” including biomolecules [1–7]. Among the various reports, one can find predominately examples of lithography on metal surfaces, and relatively fewer demonstrations on other types of inorganic substrates such as III–V semiconductor materials [3,4,6,7]. Moreover, a very limited number of studies have done a comprehensive comparison between  $\mu$ CP and DPN when the same molecular “inks” are used on III–V semiconductor surfaces [6,7].

III–V semiconductor surfaces such as gallium phosphide (GaP) are commonly used for high temperature devices and low-noise detection photodiodes [8,9]. Devices fabricated from this material have the potential to be part of a sensing platform. In order to assemble a functional sensor from such devices one needs to develop appropriate surface chemistry modification methods that facilitate the immobilization of analyte sensing moieties on the surface. Moreover the modification methods need to accommodate the size of the devices and enable site-specific localization of the sensing moieties. We recently characterized in detail the covalent attach-

ment of alkanethiols on GaP(100) substrates [10]. These studies demonstrated high alkanethiol coverage and well-packed adlayers.

In this paper, we compare the molecular patterning of alkanethiol on GaP(100) surfaces using  $\mu$ CP and DPN. The adsorbates studied were octadecanethiol (ODT), 16-mercatohexadecanoic acid (MHA), 11-amino-1-undecanethiol hydrochloride (MUAM) and mercapto-1-hexanol (MHL). The samples were characterized by atomic force microscopy (AFM), Fourier transform infrared reflection absorption spectroscopy (FT-IRRAS) and X-ray photoelectron spectroscopy (XPS). The initial goal of the work was to prove a successful transfer of the molecules onto the surface using each lithographic technique. Subsequently, the analysis studied the structure and composition of the pattern on the GaP(100) surfaces. In this study, we discuss some notable similarities and differences among the bonding, stability, organization and friction of the patterns formed by the two lithographic techniques.

### 2. Experimental section

#### 2.1. Reagents and materials

One-side polished, S-doped, n-type gallium phosphide (GaP 100) wafers were purchased from University Wafer (South Boston, MA). 1-Octadecanethiol (ODT, 98%), 16-mercatohexadecanoic acid (MHA, 90%), and mercapto-1-hexanol (MHL, 97%) were obtained from Sigma–Aldrich. 11-Amino-1-undecanethiol hydrochloride (MUAM, 90%) was acquired from Dojindo Laboratories. SYLGARD 184 silicon elastomer base and curing agent were purchased from Dow Corning Corporation (Midland, MI).

\* Corresponding author. Address: Department of Chemistry, Purdue University, West Lafayette, IN 47907, United States. Tel.: +1 765 496 3676; fax: +1 765 496 1459.

E-mail address: [albena@purdue.edu](mailto:albena@purdue.edu) (A. Ivanisevic).

## 2.2. Surface cleaning

Each n-type GaP:S wafer was cut into  $1 \times 1 \text{ cm}^2$  pieces. All samples were sonicated in pure water and ethanol for 10 min, and subsequently dried with nitrogen gas ( $\text{N}_2$ ). Each surface was cleaned in  $\text{NH}_4\text{OH}$  for  $\sim 30$  s at room temperature [11]. After the cleaning treatment the surfaces were rinsed with water and dried with  $\text{N}_2$ .

## 2.3. Microcontact printing ( $\mu\text{CP}$ )

The PDMS stamps were prepared according to the manufacturer's instructions. Prior to the stamping procedure we prepared 1 mM solutions of each alkanethiol. Prior to the stamping process each stamp was washed twice with ethanol for 15 min. Subsequently, the clean stamp was wiped using a Q-tip soaked into an alkanethiol solution. The stamp was allowed to rest for 5 min and subsequently brought into contact with the surface for 1 min. The surface was rinsed with ethanol after the stamping was done. Contact mode AFM images were collected using a Multi-Mode Nanoscope IIIa Atomic Force Microscope. Each sample was evaluated using a scan size of  $30 \times 30 \mu\text{m}^2$  and scan rate of 3.05 Hz. Images were processed using the Nanoscope III 5.12r3 software.

## 2.4. "dip-pen" Nanolithography (DPN)

All the "inks" (alkanethiols) used in the DPN procedure had concentrations of 20 mM. Single beam cantilevers from Veeco Instruments, CA (model # MSCT-AUHW and spring constant of 0.05 N/m) were modified with ODT, MHA, MUAM and MHL solutions for 15 min. A chamber was mounted around the AFM in order to control the temperature and humidity conditions. Contact mode AFM and a standard DPN protocol [3] was used in order carry out the patterning with each molecular "ink" on the GaP(100) surface.

## 2.5. Fourier transform infrared reflection absorption spectroscopy (FT-IRRAS)

We utilized a Thermo Nicolet, Nexus 670 FT-IR spectrometer for all FT-IR experiments. This single reflectance mode instrument has a narrow mercury cadmium telluride (MCT) detector. The spectrometer was cooled down using liquid  $\text{N}_2$ . The data were analyzed using the Thermo Nicolet's OMNIC software. Each data set was acquired with a resolution of  $8 \text{ cm}^{-1}$ . A background for each inter-

ested region was always collected using clean GaP(100) and subsequently subtracted from the spectra collected on the patterned sample. Two different regions were examined:  $1550\text{--}1800 \text{ cm}^{-1}$  and  $2800\text{--}3000 \text{ cm}^{-1}$ .

## 2.6. X-ray photoelectron spectroscopy (XPS)

For the XPS analysis, we prepared samples with a total patterned area of  $100 \times 100 \mu\text{m}^2$  in order to accommodate the spatial resolution of the technique. XPS data were obtained with a Kratos Ultra DLD spectrometer using monochromatic Al  $K\alpha$  radiation ( $h\nu = 1486.58 \text{ eV}$ ). The survey and high-resolution spectra were collected at fixed analyzer pass energy of 160 and 20 eV, respectively. The binding energy (BE) values refer to the Fermi level, and were referenced to C 1s at 284.80 eV. The standard deviation of the peak position associated with the calibration procedure was  $\pm 0.05 \text{ eV}$ . A commercial Kratos charge neutralizer was used to achieve a resolution of 0.6 eV measured as a full width at half maximum (FWHM) of the P 2p peaks. The data were analyzed with commercially available software, CasaXPS (version 2.313 Dev64). The individual peaks were fitted by a Gaussian/Lorentzian function after linear or Shirley type background subtraction.

## 3. Results and discussion

We began this study using standard protocols previously reported to modify surfaces by  $\mu\text{CP}$  and DPN. Identical methodology has been previously used to transfer molecular "inks" on other semiconductor surfaces [6]. The characterization we describe in this section is necessary in order to understand the physical and chemical properties of the modified GaP(100) surfaces.

### 3.1. General surface characterization

Before any patterning on the GaP substrates was done, we removed the native oxide by performing wet chemical etching with a base [11]. Four commercially available alkanethiols were patterned: ODT, MHA, MUAM and MHL. We took water contact angles of the etched and clean GaP(100), as well as surfaces modified with millimeter size alkanethiol patterns generated by  $\mu\text{CP}$ . These measurements examined the homogeneity of the substrates at the microscopic level. The water contact angles for clean GaP(100),  $\mu\text{CP-ODT}$  GaP(100),  $\mu\text{CP-MHA}$  GaP(100),  $\mu\text{CP-MUAM}$  GaP(100)

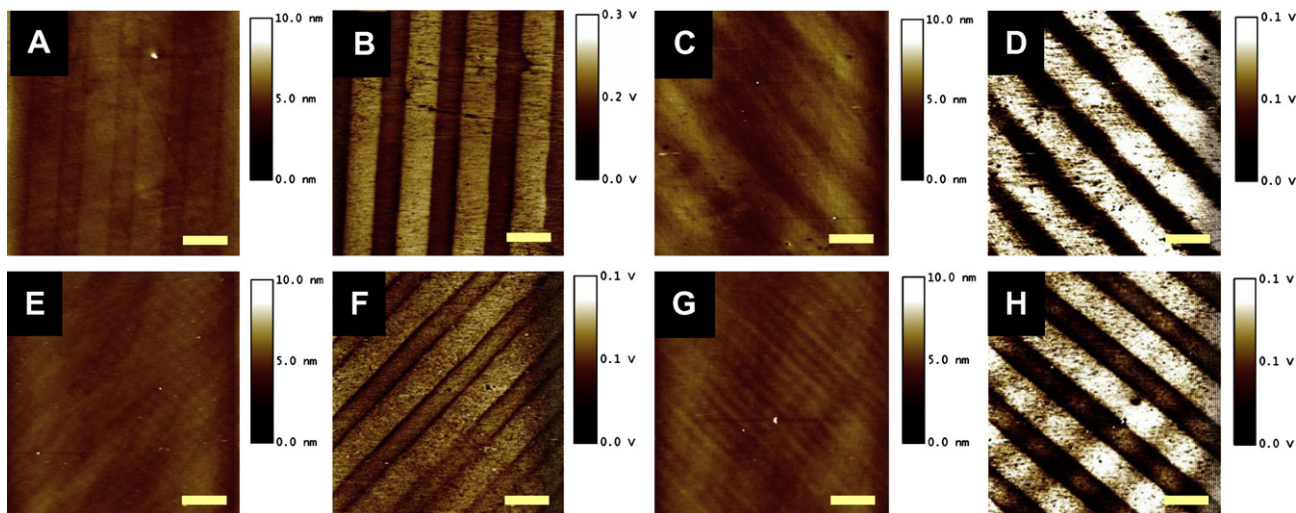


**Fig. 1.**  $\mu\text{CP}$ -Patterns of ODT (A, height and B, LFM), MHA (C, height and D, LFM), MUAM (E, height and F, LFM) and MHL (G, height and H, LFM) on GaP(100). All the images were collected with a clean tip, the scan sizes were  $30 \times 30 \mu\text{m}^2$  and the scan speed was 3.05 Hz. The scale bar is  $5 \mu\text{m}$ .

**Table 1**

Summary of the RMS values (nm) collected after analysis of areas patterned by each lithographic method

Surface	$\mu$ CP Features	DPN-features
1. ODT	$0.41 \pm 0.02$	$0.26 \pm 0.03$
2. MHA	$0.77 \pm 0.09$	$0.26 \pm 0.05$
3. MUAM	$0.47 \pm 0.06$	$0.21 \pm 0.01$
4. MHL	$0.54 \pm 0.05$	$0.31 \pm 0.03$

and  $\mu$ CP-MHL GaP(100) surfaces were  $19 \pm 1$ ,  $96 \pm 5$ ,  $60 \pm 1$ ,  $70 \pm 2$  and  $32 \pm 2$ , respectively. The hydrophobicity ( $\phi$ ) of freshly etched GaP indicated a fairly hydrophilic surface prior to any treatment. The  $\mu$ CP-modified semiconductor surface showed the following  $\phi$  increasing order:  $\phi_{\text{MHL/GaP}} < \phi_{\text{MHA/GaP}} < \phi_{\text{MUAM/GaP}} < \phi_{\text{ODT/GaP}}$ . The resultant water contact angles for the patterned adsorbates are consistent with previously published surface investigations [6,7]. AFM images, Fig. 1A–H, were done in order to understand the roughness and the pattern formation on the surface using  $\mu$ CP. The AFM height and lateral force microscopy (LFM) images showed that the pre-programmed patterns were generated on the surface. In the lateral force microscopy images darker features correspond to surface structures of relatively lower friction. We observed high friction when MHA and MHL patterns were compared with the bare surface, Fig. 1D and H. This is attributed to the high contact between the hydrophilic end groups on the surfaces and the clean tip [6,12]. Surprisingly, the more hydrophobic patterns ( $\mu$ CP-ODT and  $\mu$ CP-MUAM, Fig. 1B and F) were also observed with high friction [6,12–15]. We have repeated the patterning with these two “inks” numerous times and have always observed this result. A possible explanation for this might be in the degree of order of the molecules within the patterns. Previous detailed frictional studies in the literature have shown that “the friction measured with the AFM is on average inversely proportional to the level of order in the SAM” [7–11,6,12–18]. We also characterized each pattern by calculating the average root-mean-square (RMS) values in the patterned areas. The results are listed in Table 1. The RMS of the clean GaP(100) surface was  $0.109 \pm 0.006$  nm.  $\mu$ CP-Pattern of MHA showed the highest roughness compared with the data collected from the other types of alkanethiol patterns, possibly due to more non-homogeneously ordered monolayers on the surface [10].

The second method that we used to demonstrate molecular patterning on GaP(100) was DPN, Fig. 2. All patterning steps were per-

formed at the humidity of  $\sim 32$ – $34\%$  and at temperature of  $24^\circ\text{C}$ . Features generated with ODT and MHA are shown in Fig. 2A–D, where the size of the squares is  $3 \times 3 \mu\text{m}^2$  and was generated by using a speed of 2 Hz. The rectangles of MUAM molecules, Fig. 2E and F, were done using a ratio of 16:1 as the scan size and a scan speed of 1.5 Hz. The writing speed for the long molecular lines ( $5 \mu\text{m}$ ) composed of MHA was  $15.25 \mu\text{m/s}$ , Fig. 2G and H. The AFM images of each pattern were taken with a clean tip after they were dried for 1 h. The RMS values associated with each type of pattern are summarized in Table 1. The LFM images confirmed the difference in friction which depends on the interaction of the clean tip with the end functional group of the pattern and the bare tip surface. MHA and MHL DPN patterns presented higher friction than the ODT and MUAM DPN samples. These results were similar to the contrast seen in previous surface investigations [3–7,19,20]. The initial characterization confirm the ability to successfully pattern GaP(100) surfaces on the micron and nanometer scale. In order to understand the chemical composition and gather deeper understanding of the organization of the molecules within the patterns we carried out further spectroscopic analysis using XPS and FT-IRRAS.

### 3.2. Elemental composition of the patterns on GaP(100) surfaces: XPS analysis

XPS is a powerful technique, which provides information about the chemical composition of the micro-scale SAM patterns and molecular adlayers [21,22]. We investigated each type of alkanethiol modification by XPS using a micron-size alignment indicator in order to take spectra from a specific lithographic pattern. We analyzed the core level spectra of gallium (Ga 3d and Ga  $2p_{3/2}$ ), phosphorus (P 2p), sulfur (S 2p), carbon (C 1s), nitrogen (N 1s) and oxygen (O 1s). Each spectrum was fitted assuming a Gaussian/Lorentzian line shape. The curve fitting is particularly important for the S 2p and N 1s analysis because these photoelectron transitions overlap with the Ga 3s and Ga Auger peaks, respectively [10]. The peak positions for the clean,  $\mu$ CP- and DPN-modified GaP(100) are summarized in Table 2.

High-resolution core level spectra of the S 2p/Ga 3s region were collected in order to rationalize each patterning modification on GaP(100), Fig. 3. An asymmetric peak at 159.9 eV is representative of Ga 3s from the clean GaP (see the light turquoise peak in Fig. 3). After  $\mu$ CP and DPN of the alkanethiols on the surface, the S 2p doublet peaks at ca. 162 eV became detectable [10,23–28]. This peak

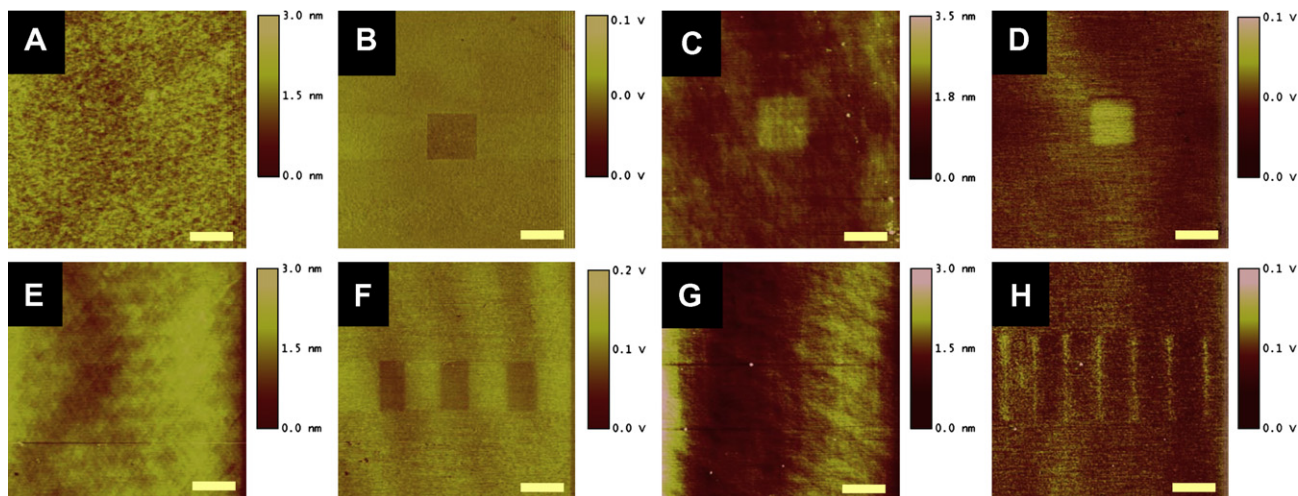


**Fig. 2.** DPN patterns of ODT (A, height and B, LFM), MHA (C, height and D, LFM), MUAM (E, height and F, LFM) and MHL (G, height and H, LFM) on GaP(100). All the images were collected with a clean tip, the scan sizes were  $15 \times 15 \mu\text{m}^2$  and the scan speed was 4.05 Hz. The scale bar is  $3 \mu\text{m}$ .

**Table 2**  
Summary of the peak positions of S 2p/Ga 3s, C 1s and N 1s obtained on different samples

Peak assignments	Binding energy (eV)									
	Clean GaP(100)	ODT/GaP(100)		MHA/GaP(100)		MUAM/GaP(100)		MHL/GaP(100)		
			$\mu$ CP	DPN	$\mu$ CP	DPN	$\mu$ CP	DPN	$\mu$ CP	DPN
S 2p <sub>3/2</sub>										
S <sup>+</sup> bound to Ga		161.3	161.8	161.3	161.8	161.6		161.7		161.3
S <sup>-</sup> bound to SO <sub>x</sub>								168.5		
Ga 3s										
GaP	159.9	160.1		160.2		160.2		160.1		
C 1s										
C–C	284.8	284.8	284.8	284.8	284.8	284.8	284.8	284.8	284.8	284.8
C–OH										
HO–C=O				288.9	288.9					
C–N						286.3		285.7		
N 1s										
Ga 3d (Auger)	390.3, 392.3, 393.9,					390.6, 392.6, 394.1,		390.4, 392.3, 393.9,		
L <sub>3</sub> M <sub>45</sub> M <sub>45</sub>	395.6, 399.1					395.8, 399.0		395.6, 398.1		
NH <sub>2</sub> /NH <sub>3</sub> <sup>+</sup>						400.0		399.7		

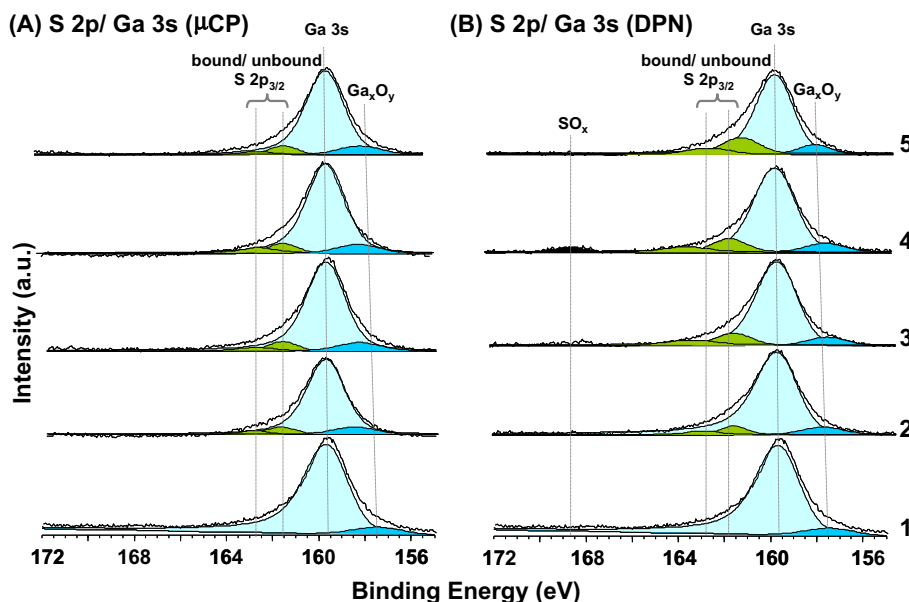


**Fig. 3.** High resolution XPS spectra of S 2p/Ga 3s region after (A)  $\mu$ CP and (B) DPN: (1) freshly etched GaP(100), (2) GaP(100) patterned with ODT, (3) GaP(100) patterned with MHA, (4) GaP(100) patterned with MUAM and (5) GaP(100) patterned with MHL.

position is characteristic of covalently bond sulfur to the substrate. These peaks are plotted in lime color and the spin-orbital doublet splitting is 1.15 eV, spectra 2–5 in Fig. 3. Regardless of which patterning technique was used, we recorded a weak S signal. On samples patterned with MUAM by DPN, Fig. 3, spectrum 4, an additional component is detected at  $\sim$ 169 eV which is attributed to oxidized sulfur [23–25]. In order to have additional information about the composition of the patterns generated by each lithographic technique, the C 1s and N 1s core level spectra were analyzed.

The C 1s core level spectra are represented in Fig. 4. Freshly etched GaP(100) substrates had some carbon contamination due to a short exposure to air. After the preparation of the molecular patterns by both lithographic approaches, the C 1s peak intensity increased in comparison with the clean surface. It is important to note that the C 1s intensity was higher for the surfaces patterned by  $\mu$ CP than for the ones modified by DPN. We also would like to note that in the case of a surface modified by DPN, the XPS spot of analysis was bigger than the DPN pattern and therefore the anal-

ysis covered some non-functionalized (i.e. clean) fraction of the surface. The surfaces patterned by DPN with ODT were more susceptible to carboxylic acid contaminates compared with samples that were modified with other adsorbates [10]. Samples modified with the MHA ink and each technique, the deconvolution of the spectra revealed OH–C=O and C–OH component that were detected at  $\sim$ 288.9 eV and  $\sim$ 286.0 eV, respectively. Surfaces functionalized with MUAM using  $\mu$ CP and DPN showed a C 1s component at 286.3 eV and 285.7, respectively. This component is consistent with the presence of nitrogen bonded species and was confirmed by the analysis of the N 1s core level spectra.

In Fig. 5, the N 1s peak overlaps with the Ga L<sub>3</sub>M<sub>45</sub>M<sub>45</sub> Auger lines [29]. The Ga L<sub>3</sub>M<sub>45</sub>M<sub>45</sub> Auger lines were observed for clean GaP(100) and for all patterned surfaces. The Auger line shape was extracted from the spectra obtained from the clean surface. Subsequently the Auger line constraint was used to deconvolute the N 1s peak. A peak attributed to N 1s at  $\sim$ 400 eV can be assigned to C–N and NH<sub>2</sub>/NH<sub>3</sub><sup>+</sup> species from MUAM on surfaces patterned by

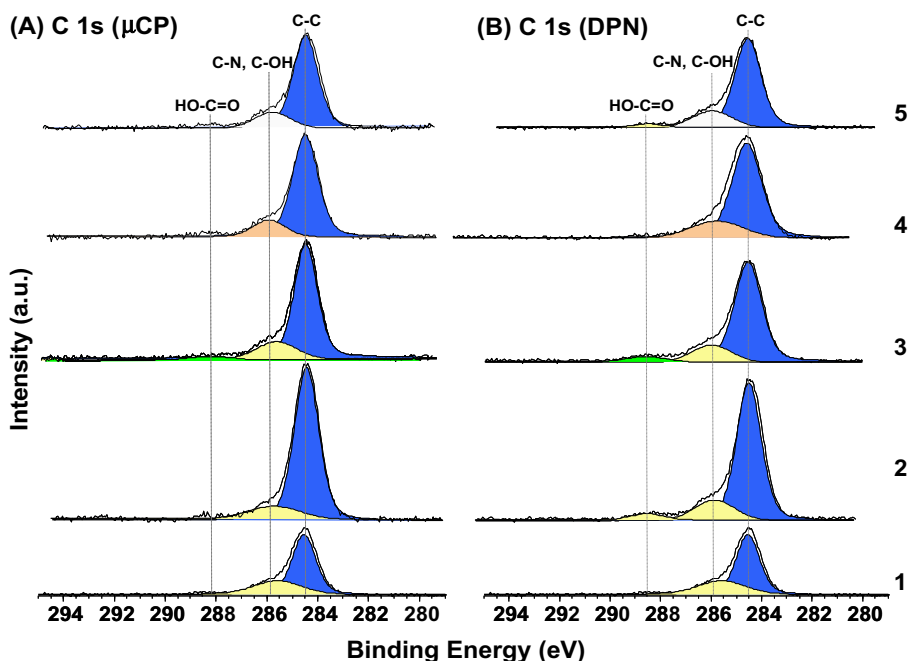


**Fig. 4.** High resolution XPS spectra of the C 1s region after (A)  $\mu$ CP and (B) DPN: (1) clean GaP, (2)  $\mu$ CP/DPN-ODT on GaP(100), (3)  $\mu$ CP/DPN-MHA on GaP(100), (4)  $\mu$ CP/DPN-MUAM on GaP(100) and (5)  $\mu$ CP/DPN-MHL on GaP(100).

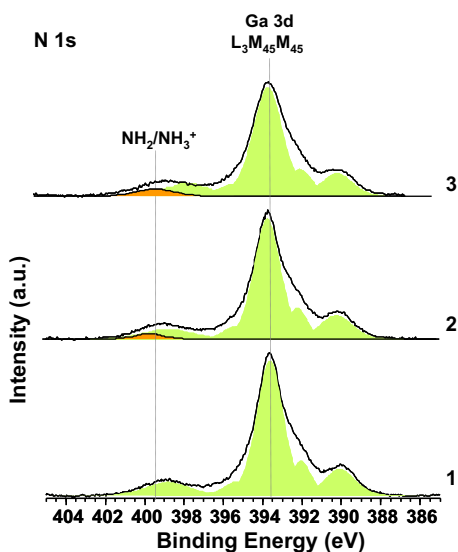


**Fig. 5.** Deconvoluted XPS spectra of N 1s region of the following samples: (1) clean GaP(100), (2) GaP(100) after patterning of MUAM by  $\mu$ CP and (3) GaP(100) after patterning of MUAM by DPN.

each method. All the XPS data we collected confirmed the successful transfer of the chosen “inks” onto the surface and provided evidence for the formation of a bond to the GaP(100) surface.

### 3.3. Chemical species arrangement on GaP(100) surfaces: FT-IRRAS characterization

In order to assess the order level of the molecule layer patterning by each lithographic method, FT-IRRAS data were collected. A low frequency region ( $1550\text{--}1800\text{ cm}^{-1}$ ) and a high frequency ( $2800\text{--}3000\text{ cm}^{-1}$ ) were examined, as shown in Figs. 6 and 7. As expected from ODT and MHL chemical structures, no peak in the

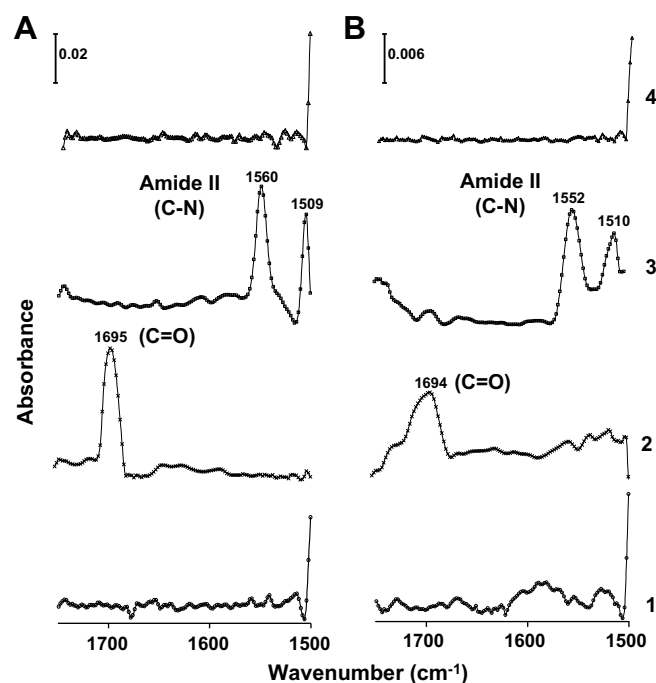


**Fig. 6.** FT-IRRAS spectra of the region between  $1750$  and  $1500\text{ cm}^{-1}$  for samples modified by (A)  $\mu$ CP and (B) DPN. The following samples are presented: (1) ODT-patterned/GaP(100); (2) MHA-patterned/GaP(100); (3) MUAM-patterned/GaP(100) and (4) MHL-patterned/GaP(100).

low frequency region was observed for the surfaces patterned by each technique, as shown in Fig. 6 (spectra 1 and 4). Surfaces patterned with MHA (Fig. 6, spectrum 2), showed a peak at  $1695\text{ cm}^{-1}$  and  $1694\text{ cm}^{-1}$  after  $\mu$ CP and DPN modifications, respectively. This peak is due to the presence of C=O moieties on the surface [6,10,27,30]. We recorded evidence for the presence of MUAM on the surface after the lithographic procedures due to the appearance

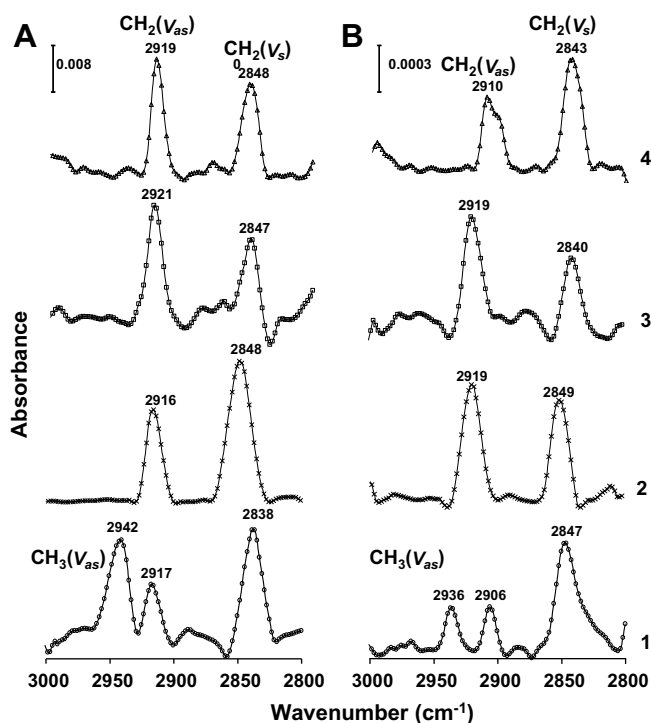


**Fig. 7.** FT-IRRAS spectra of the region between 3000 and 2800  $\text{cm}^{-1}$  for samples modified by (A)  $\mu\text{CP}$  and (B) DPN. The following samples are presented: (1) ODT-patterned/GaP(100); (2) MHA-patterned/GaP(100); (3) MUAM-patterned/GaP(100) and (4) MHL-patterned/GaP(100).

of amide II peaks [10,31]. These peaks were at 1509/1510  $\text{cm}^{-1}$  on surfaces functionalized by  $\mu\text{CP}$  and at 1552/1560  $\text{cm}^{-1}$  on DPN-modified surfaces.

FT-IRRAS experiments were also used to study the orientation of the alkanethiol molecules on the surfaces. In order to gather this information, we analyzed the high frequency region (2800–3000  $\text{cm}^{-1}$ ). The position of the symmetric  $\text{CH}_2$  stretch is used to assess if the packing of the molecules within the patterns is in a liquid-like or crystalline-like state [10,21,27,30–32]. The symmetric  $\nu_s(\text{CH}_2)$  and asymmetric  $\nu_{as}(\text{CH}_2)$  stretching mode of  $\text{CH}_2$  for alkanethiol solutions were positioned at  $\sim 2851$ – $2855$   $\text{cm}^{-1}$  and 2924–2931  $\text{cm}^{-1}$ , respectively [10]. Fig. 7A shows the  $\nu_{as}(\text{CH}_2)/\nu_s(\text{CH}_2)$  bands for microcontact printing patterns of the alkanethiol molecules on GaP(100). These peaks are located at 2917  $\text{cm}^{-1}$ /2838  $\text{cm}^{-1}$ , 2916  $\text{cm}^{-1}$ /2848  $\text{cm}^{-1}$ , 2921  $\text{cm}^{-1}$ /2847  $\text{cm}^{-1}$ , and 2919  $\text{cm}^{-1}$ /2848  $\text{cm}^{-1}$  for ODT, MHA, MUAM and MHL, respectively. The asymmetric  $\nu_{as}(\text{CH}_2)$ /symmetric  $\nu_s(\text{CH}_2)$  vibrations for ODT, MHA, MUAM and MHL DPN samples were positioned at 2906  $\text{cm}^{-1}$ /2847  $\text{cm}^{-1}$ , 2919  $\text{cm}^{-1}$ /2849  $\text{cm}^{-1}$ , 2919  $\text{cm}^{-1}$ /2840  $\text{cm}^{-1}$  and 2910  $\text{cm}^{-1}$ /2843  $\text{cm}^{-1}$ , respectively. The data we gathered support the notion that the patterns of the alkanethiol molecules are in a crystalline-like state on the GaP(100) [10,27,30–32]. It is worthy to note that the biggest difference we recorded between the organization of the patterns on each surface when a different lithographic approach was utilized was in the case of the ODT ink. The FT-IRRAS data indicates that the GaP surfaces patterned by DPN with this ink produced more ordered monolayers

compared to the ones generated by  $\mu\text{CP}$ . This observation is consistent with the AFM data discussed earlier.

#### 4. Summary

This study demonstrated a complete qualitative characterization of alkanethiol patterning on GaP(100) surfaces using  $\mu\text{CP}$  and DPN. The AFM data showed well-defined structures at optimal conditions by both lithographic techniques. The XPS data allowed us to understand the elemental composition of GaP(100) surfaces modified by four different “inks”. A small amount of sulfur S was observed on surfaces functionalized by both DPN and  $\mu\text{CP}$  and a covalent attachment to the surface was confirmed. FT-IRRAS analysis showed that there are differences in the organization of the molecules on the surface after each lithographic modification but they are dependent upon the chosen molecular “ink”.

#### Acknowledgment

This work was supported by NSF under CHE-0614132.

#### References

- [1] Y. Xia, J.A. Rogers, K.E. Paul, G.M. Whitesides, *Chem. Rev.* 99 (1999) 1823.
- [2] K.L. Christman, V.D. Enriquez-Rios, H.D. Maynard, *Soft Matt.* 2 (2006) 928.
- [3] R.D. Piner, J.Z. Feng-Xu, S. Hong, C.A. Mirkin, *Science* 283 (1999) 661.
- [4] A. Ivanisevic, C.A.J. Mirkin, *Am. Chem. Soc.* 123 (2001) 7887.
- [5] D.L. Wilson, R. Martin, S. Hong, M. Cronin-Golomb, C.A. Mirkin, D.L. Kaplan, *PNAS* 98 (2001) 13660.
- [6] Y. Cho, A. Ivanisevic, *Langmuir* 22 (2006) 8670.
- [7] H.P. Wampler, D.Y. Zemlyanov, A. Ivanisevic, *Phys. Chem. C Lett.* 111 (2007) 17989.
- [8] K.Z. Liu, Y. Suzuki, Y. Fukuda, *Surf. Inter. Anal.* 36 (2004) 966.
- [9] A.L. Beck, B. Yang, S. Wang, C.J. Collins, J.C. Campbell, A. Yulius, A. Chen, J.M. Woodall, *IEEE J. Quant. Electron.* 40 (2004) 1695.
- [10] R. Flores-Perez, D.Y. Zemlyanov, A.J. Ivanisevic, *Phys. Chem. C* 112 (2008) 2147.
- [11] H. Morota, S.J. Adachi, *Appl. Phys.* 100 (2006) 054904.
- [12] J.R. Hampton, A.A. Dameron, P.S.J. Weiss, *Am. Chem. Soc.* 128 (2006) 1648.
- [13] K. Sasaki, Y. Koike, H. Azebara, H. Hokari, M. Fujihira, *Appl. Phys. A* 66 (1998) S1275.
- [14] Y. Xia, G.M. Whitesides, *Langmuir* 13 (1997) 2059.
- [15] T. Auletta, B. Dordi, A. Mulder, A. Sartori, S. Onclin, C.M. Bruinink, M. Peter, C.A. Nijhuis, H. Beijleveld, H. Schonherr, G. Julius, A. Casnati, R. Ungaro, B.J. Ravoo, J. Huskens, D.N. Reinhoudt, *Angew. Chem. Int. Ed.* 43 (2004) 369.
- [16] M. Castronovo, F. Bano, S. Raugei, D. Scaini, M. Dell'Angela, R. Hudej, L. Casalis, G.J. Scoles, *Am. Chem. Soc.* 129 (2007) 2636.
- [17] J.E. Houston, C.M. Doelling, T.K. Vanderlick, Y. Hu, G. Scoles, I. Wenzl, T.R. Lee, *Langmuir* 21 (2005) 3926.
- [18] J. Pflaum, G. Bracco, F. Schreiber, R. Colorado, O.E. Shmakova, T.R. Lee, G. Scoles, A. Kahn, *Surf. Sci.* 498 (2002) 89.
- [19] S. Hong, J. Zhu, C.A. Mirkin, *Science* 286 (1999) 523.
- [20] D. Bullen, S.-W. Chung, X. Wang, J. Zou, C.A. Mirkin, C. Lui, *Appl. Phys. Lett.* 84 (2004) 789.
- [21] R.G. Nuzzo, L.H. Dubois, D.L.J. Allara, *Am. Chem. Soc.* 112 (1990) 558.
- [22] C.Y. Lee, G.M. Harbers, D.W. Grainger, L.J. Gamble, D.G.J. Castner, *Am. Chem. Soc.* 129 (2007) 9429.
- [23] Y. Jun, X.-Y. Zhu, J.W.P. Hsu, *Langmuir* 22 (2006) 3627.
- [24] C.L. McGuiness, A. Shaporenko, C.K. Mars, S. Uppili, M. Zharnikov, D.L.J. Allara, *Am. Chem. Soc.* 128 (2006) 5231.
- [25] C.L. McGuiness, A. Shaporenko, M. Zharnikov, A.V. Walker, D.L.J. Allara, *Phys. Chem. C* 111 (2007) 4226.
- [26] Y. Suzuki, N. Sanada, M. Shimomura, Y. Fukuda, *Appl. Surf. Sci.* 235 (2004) 260.
- [27] Y. Cho, A.J. Ivanisevic, *Phys. Chem. B* 109 (2005) 12731.
- [28] H.H. Park, A.J. Ivanisevic, *Phys. Chem. C* 111 (2007) 3710.
- [29] P. Staib, J.P. Contour, J.J. Massies, *Vacuum Sci. Technol. A* 3 (1985) 1965.
- [30] R. Flores-Perez, A. Ivanisevic, *Appl. Surf. Sci.* 253 (2007) 4176.
- [31] K. Nakano, T. Sato, M. Tazaki, M. Takagi, *Langmuir* 16 (2000) 2225.
- [32] Z. Li, S. Chang, R.S. Williams, *Langmuir* 19 (2003) 6744.